

A Nonflammable Diethyl Ethylphosphonate-based Electrolyte Improved by Synergistic Effect of Lithium Difluoro(oxalato)borate and Fluoroethylene Carbonate

Lihua Jiang ^a, Yuan Cheng ^a, Jinhua Sun ^a, Martin Winter ^{b, c}, Isidora Cekic-Laskovic ^b,

^{*}, Qingsong Wang ^{a, *}

^a *State Key Laboratory of Fire Science, University of Science and Technology of China,*

Huangshan Road 443, 230026, Hefei, China

^b *Helmholtz Institute Münster, IEK-12, Forschungszentrum Jülich GmbH,*

Corrensstrasse 46, 48149, Münster, Germany

^c *University of Münster, MEET Battery Research Center, Institute of Physical*

Chemistry, Corrensstrasse 46, 48149, Münster, Germany

*Email: pinew@ustc.edu.cn; i.cekic-laskovic@fz-juelich.de

Abstract

The vital physical and chemical properties of the lithium conducting salt, solvent/co-solvent and functional additive determine the overall properties and performance of the resulting electrolyte formulation. Explorations on right combinations of the carefully selected electrolyte components are expected to further balance the electrochemical and safety performances of chosen electrolyte formulations in given cell chemistries. In this study, a new nonaqueous aprotic electrolyte is designed by using lithium difluoro (oxalato) borate (LiODFB) as conducting salt, diethyl ethylphosphonate (DEEP) as solvent, and fluoroethylene carbonate (FEC) as co-solvent to achieve a nonflammable electrolyte formulation with competent electrochemical performance. The LiODFB and FEC are

believed to take part in complex interfacial interactions with a synergistic effect. NCM811 || Li cells using the optimized electrolyte formulation of 1.3 M LiODFB/DEEP 30% FEC exhibits a stable long-term cycling at 1.0 C with a reversible average specific discharge capacity of 169.45 mAh g⁻¹ during 100 cycles, which is comparable to cells using commercial electrolytes. Furthermore, the 1.3 M LiODFB/DEEP 30% FEC electrolyte shows good thermal stability and effectively reduces the heat generation during thermal decomposition of NCM811 cathode. The results provide a good reference for the design of next generation of safe, nonflammable electrolytes for lithium-based battery application.

Keywords: Lithium-based battery safety; Nonflammable electrolyte; Lithium difluoro (oxalato) borate; Diethyl ethylphosphonate electrolyte solvent; Synergistic effect.

1. Introduction

In response to the global climate change, many countries around the world are advocating the application of clean energy to replace traditional fossil fuels to reduce the emissions of greenhouse gases. Driven by the transformation of the global energy structure, the most representative changes should be the leap development of electric vehicles and electrochemical energy storage industries[1]. Due to the advantages of portability, long cycle life and high energy density, lithium-based batteries have become one of the most common energy storage devices to overcome the discontinuity of some clean energy such as wind energy, water energy, solar energy, etc[2-4]. However, the frequent fire and even explosion accidents of electric vehicles and energy storage power stations caused by the thermal runaway of lithium-based batteries have become a technical obstacle for the long-term development of the industry[5, 6], thus the fire safety of lithium-ion batteries is the most urgent problem which needs to be solved at present[7, 8]. The safe application of lithium-based batteries is strongly limited by the internal

flammable components, especially the organic carbonate-based formulations as state of the art electrolytes with low flash point. A lot of studies have shown that the thermal runaway of lithium-based batteries can be interpreted by a series of chain reactions[9-11]. Heat accumulation will firstly initiate the side reactions such as the thermal decomposition of solid electrolyte interface (SEI) film, causing the battery temperature to rise further. Reactions between anode and electrolyte, the melting of separator, the decomposition of cathode, and the decomposition of electrolyte will be initiated sequentially[11]. The internal short circuit between anode and cathode will release massive electric energy and possibly ignite the electrolyte. Since the electrolyte is almost involved in multiple thermal runaway chain reaction steps, optimizing the chemical composition of electrolytes is considered as one of the most effective means to improving the intrinsic safety of batteries[12, 13]. Adding flame retardant additives/co-solvents into conventional electrolytes is a direct way to improve the flash point but the retardant effect will be restricted by a low addition, while a large amount of addition will cause seriously degeneration of the electrochemical performance[14]. Solid state electrolytes can avoid the occurrence of internal short circuits, which can significantly improve the battery safety. However, the ionic conductivity of solid state electrolytes at room temperature and their interfacial contact with electrode is still poor for the current stage, which limits their practical applications at present[15].

Recent studies reported the strategy to use flame retardants as electrolyte solvents to formulate completely nonflammable electrolyte, and an effective SEI film formation by using high salt-to-solvent ratio which reduces free solvent molecules[16]. The most representative formulation is the combination of phosphate flame retardants such as trimethyl phosphate (TMP)[14] and triethyl phosphate (TEP)[17] with lithium salt possessing higher thermal stability compared to lithium hexafluorophosphate (LiPF_6)

such as lithium bis(fluorosulfonyl)imide (LiFSI) and lithium bis(trifluoromethane sulfonimide) (LiTFSI) [18, 19]. For example, by controlling the molar ratio of salt to solvent (MR) within the electrochemical stability threshold of the solvent ($>1:2$), Zeng et al.[20] identified a nonflammable TEP-based electrolyte containing fluoroethylene carbonate (FEC) and lithium bis(oxalate)borate (LiBOB) in which the molar ratio of LiFSI to TEP is 1:2 (molar concentration is about 2.2 mol L^{-1}). It is worth noting that under high conducting salt to solvent ratio, most of the TEP molecules are complexed with Li^+ ions, and there are no free solvent molecules causing a negative shift in the solvent reduction potential to inhibit the electrochemical decomposition of TEP molecules[20, 21]. However, highly concentrated electrolytes also bring about a series of problems such as a significant increase in cost, high viscosity, low conductivity, and a deterioration in wettability[16]. One solution could be the introduction of an inert solvent to ‘dilute’ the concentrated electrolyte[22, 23]. Chen et al.[24] added bis(2,2,2-trifluoroethyl) ether (BTFE), as electrochemically inert and poor solvent of lithium salt, which can maintain the solvated structure of high concentrated electrolyte thus forming a localized high-concentration electrolyte, to dilute the 3.2 mol L^{-1} LiFSI/TEP electrolyte. However, the compatibility of diluted electrolyte towards high-voltage cathodes may be restricted[25]. The physical and chemical characteristics of the lithium salt, solvent(s) and functional additive(s) determine the overall properties of the electrolyte and significantly impact the electrochemical performance[16]. Explorations on more suitable combinations of the electrolyte components are expected to further improve the compatibility of nonflammable phosphate-based electrolytes. At present, few studies have paid attention to the impact of the type of lithium salts on the electrochemical performance of phosphate-based electrolytes[26-28]. Among alternative lithium salts to the traditional LiPF_6 , lithium difluoro(oxalato)borate (LiODFB) combines the structures of LiBOB and lithium

tetrafluoroborate (LiBF_4) showing the advantages of both LiBOB and LiBF_4 [29, 30], such as good film-forming properties, high temperature performance and passivation effect of aluminum current collectors[31-33]. For current studies, LiODFB is widely used as an electrolyte additive, but there are few investigations on its application as an electrolyte single salt[34].

In this study, we propose a new electrolyte formulation by using diethyl ethylphosphonate (DEEP) as flame retardant solvent, FEC as co-solvent and LiODFB as single salt to formulate a nonflammable electrolyte with a wide electrochemical stability window and good compatibility with $\text{LiNi}_{0.8}\text{Co}_{0.1}\text{Mn}_{0.1}\text{O}_2$ (NCM811) and lithium metal electrodes. LiODFB and FEC are believed to have a synergistic effect which can significantly improve the electrochemical performance of the resulting cell chemistry[35, 36]. Different concentrations of LiODFB and FEC were investigated in detail on the influence of the electrochemical performance for NCM811||Li cells to realise a comparable long galvanostatic cycling performance with commercial organic carbonate electrolyte. This work can provide a good reference for the design of next generation of safe electrolyte for lithium-based battery application.

2. Experimental

2.1. Preparation

Commercial 1.0 M $\text{LiPF}_6/\text{EC}/\text{DEC}$ (3:7, wt.%) (BASF SE, Germany) electrolyte was used as the standard electrolyte. All chemicals, as components of the nonflammable electrolyte, were commercially purchased without additional chemical treatment. DEEP (abcr, 98%) was used as a main solvent and FEC (TCL, 98%) was used as a co-solvent. Different concentrations of LiODFB (abcr, 99%) lithium salt were completely dissolved in the DEEP and FEC mixture in an argon-filled glove box (Mbraun, Germany, H_2O and $\text{O}_2 < 0.1$ ppm). Cathode material NCM811, polyvinylidene fluoride (PVDF) and

acetylene black, provided by the battery line of Münster electrochemical energy technology (MEET) battery research center, were mixed in a mass ratio of 8: 1: 1. The mixture was thereafter mixed with *N*-methyl pyrrolidone solvent to obtain an homogeneous slurry, which was further coated on an aluminum collector. The prepared electrodes were dried in a vacuum oven under 80 °C for 10 hours, the average active mass loading of the resulting electrodes is about 2.2 mg cm⁻².

2.2. Electrochemical characterization

CR2032 coin and Swagelok® cells were assembled to investigate electrochemical performance of the above described cell chemistry. For CR2032 coin cells assembly, NCM811 (12 mm) was used as working electrode (WE) and lithium foil (12 mm) the counter electrode (CE), whereas separator (Celgard 2500, 14 mm) was used between WE and CE and volume of 60 µl electrolyte was added to wet the electrode and separator. For linear sweep voltammetry (LSV), Swagelok cells in a three electrodes setup were used, with platinum (1 mm) as WE, lithium foil as CE (5 mm) and reference electrode (RE, 12 mm). Glass microfiber filter (GF/D Whatman) was used as the separator; the separator (14 mm) between WE and CE was wetted with 150 µl electrolyte, and the separator (10 mm) close to RE was wetted with 50 µl electrolyte.

The coin cells were used to conduct galvanostatic cycling and rate performance tests on the battery tester (MACCOR Series 4000, America) under 20 °C. For long term cycling test, cells were pre-cycled with a current rate of 0.2 C for three cycles and followed by 100 charge/discharge cycles at 1.0 C, in the voltage range from 2.8 to 4.5 V. For rate performance test, the cells were cycled with the current rate of 0.2 C, 0.5 C, 1.0 C, 1.5 C, 2.0 C, respectively.

LSV was conducted using VSP potentiostat (Biologic, France) to evaluate the electrochemical stability window of the considered electrolytes. Before each test, the platinum WE was polished with aluminum hydroxide suspension polishing solution to remove the oxide film on surface. In the reduction stability test, the scan voltage range was set from the open circuit potential to 1.0 V (relative to $\text{Li} \mid \text{Li}^+$), and in the oxidation stability test, the scan voltage range was set from the open circuit potential to 6.0 V (relative to $\text{Li} \mid \text{Li}^+$), the scan rate was 1.0 mV s^{-1} . The arbitrary limiting current for determination of electrolyte stability was set to 0.01 mA cm^{-2} .

The ionic conductivity of the considered electrolytes was determined using the MCS10 multi-channel conductivity meter (Biologic, France) at following temperatures: 20°C , 25°C and 30°C . The electrolyte was added in a conductivity cell with two platinum electrodes (Amel Glassware), the cell constant was calibrated by the aqueous 0.01 M KCl solution (1.413 mS cm^{-1} at 25°C)[37, 38].

2.3. Characterization analysis

Coin cells, galvanostatically cycled for 100 charge/discharge cycles with different electrolytes were disassembled and harvested electrodes for further surface morphology and chemical composition analysis. The obtained electrodes were washed by dimethyl carbonate (DMC) for three times to remove the residual electrolyte on the electrode surface. The surface morphology of the electrode was observed by the scanning electron microscopy (SEM, Zeiss Auriga crossbeam workstation, Germany), the accelerating voltage was 3 kV and the working distance was 3 mm , using the InLens detector.

2.4. Thermal stability determination

Thermal stability of the formulated electrolytes was evaluated by burning test and microcalorimetric analysis. For burning test, 500 μl electrolyte was added to a glass fiber separator (200 mm) and then ignited by flame to intuitively evaluate the flammability. For accurate thermal stability analysis, a C80 microcalorimeter (Setaram, France) was used to detect the thermal decomposition temperature and heat flow. The test temperature range was set from room temperature to 300 $^{\circ}\text{C}$ with a heating rate of 0.2 $^{\circ}\text{C min}^{-1}$. Before the C80 tests, cells with different electrolytes were pre-cycled with a current rate of 0.2 C for three cycles and finally charged to the cut off voltage. The fully charged cells were disassembled in the glove box, and the harvested electrodes were washed by DMC with three times to remove the residual electrolyte on the surface, the dried electrodes were wetted with the considered electrolytes with a mass ratio of 1:1 and encapsulated in a C80 reaction tank under argon atmosphere for thermal stability tests.

3. Results and discussion

In order to evaluate the electrochemical stability of DEEP as an electrolyte solvent, LSV was conducted in Swagelok cells. The obtained linear sweep voltammograms (Fig.1) show that the oxidative stability potential of DEEP can be up to 4.65 V vs. $\text{Li} | \text{Li}^{+}$, and no distinct reduction peaks are observed, which means that DEEP is a good alternative solvent for electrolytes. LiODFB were subsequently dissolved in DEEP to formulate the 1.0 M LiODFB/DEEP electrolyte. The linear sweep voltammogram of the 1.0 M LiODFB/DEEP electrolyte shows that the addition of LiODFB leads to a narrow electrochemical stability window compared to pure DEEP. The oxidative stability potential of the 1.0 M LiODFB/DEEP electrolyte is only 4.0 V, and several obvious reductive decomposition peaks are observed, which will limit the operating potential range of cells. According to literature and our previous studies[39], FEC is a good additive

/co-solvent to suppress side oxidation and reduction reactions to improve the electrochemical stability of electrolyte and the interface compatibility between electrolyte and electrode[17, 39, 40]. On this basis, 10% FEC was introduced into the 1.0 M LiODFB/DEEP electrolyte as a co-solvent to inhibit adverse side reactions. The linear sweep voltammogram of the 1.0 M LiODFB/DEEP 10% FEC electrolyte shows that the electrochemical decomposition reactions of the 1.0 M LiODFB/DEEP electrolyte on both the oxidation and reduction directions can be well suppressed by adding FEC, the oxidative stability potential returns to 4.65 V, and the reductive decomposition peaks also disappear. Therefore, the 1.0 M LiODFB/DEEP 10% FEC electrolyte exhibits a wide electrochemical stability window (0-4.65 V), implying that it is a potential candidate formulation for Li-ion battery electrolyte.

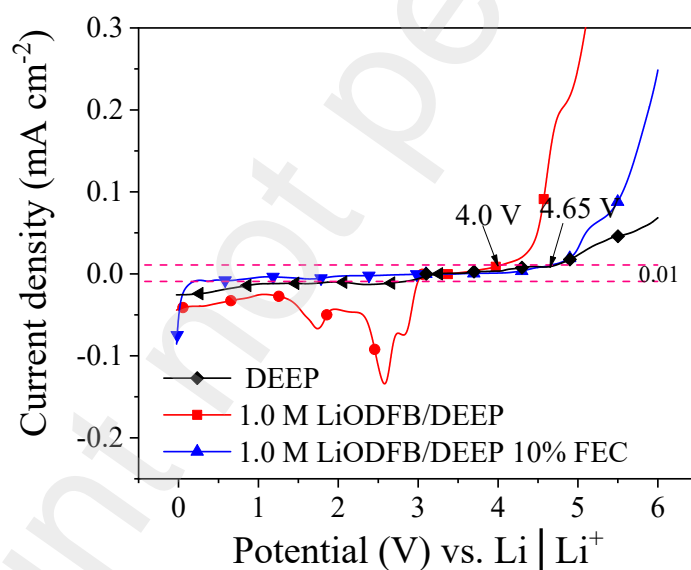


Fig.1 Linear sweep voltammograms of pure DEEP, 1.0 M LiODFB/DEEP and 1.0 M LiODFB/DEEP 10% FEC

The electrolyte was applied into the NCM811 || Li coin cell system to evaluate the long-cycling stability, the charge-discharge voltage range was set at 2.8-4.5 V, according

to the determined electrochemical stability window. Fig.2 compares the reversible specific discharge capacity and Coulombic efficiency of cells containing standard (1.0 M $\text{LiPF}_6/\text{EC}/\text{DEC}$ (3:7, wt.%)), 1.0 M $\text{LiODFB}/\text{DEEP}$ and 1.0 M $\text{LiODFB}/\text{DEEP}$ 10% FEC electrolytes. The results show that cells containing the 1.0 M $\text{LiODFB}/\text{DEEP}$ electrolyte display a comparable specific discharge capacity with cells containing standard electrolyte, while the average Coulombic efficiency of cells containing the 1.0 M $\text{LiODFB}/\text{DEEP}$ electrolyte during 100 charge/discharge cycles amounts to 98.02%. By combining with the linear sweep voltammograms, the electrochemical stability window of the 1.0 M $\text{LiODFB}/\text{DEEP}$ electrolyte cannot cover the operating potential range of the $\text{NCM811} \parallel \text{Li}$ coin cell, the oxidative decomposition reaction over 4.0 V of the 1.0 M $\text{LiODFB}/\text{DEEP}$ electrolyte and the reductive reaction in the anodic cut-off potential direction will lead to a decrease in Coulombic efficiency. After introducing 10% of FEC, the Coulombic efficiency of $\text{NCM811} \parallel \text{Li}$ cells containing the 1.0 M $\text{LiODFB}/\text{DEEP}$ 10% FEC electrolyte during 100 charge/discharge cycles is improved to 99.53%, which can be attributed to the effective preventing effect of FEC on the decomposition of electrolyte, making the electroplating process of Li^+ more effective and forming uniform interface film[14, 41]. However, the cells containing the 1.0 M $\text{LiODFB}/\text{DEEP}$ 10% FEC electrolyte exhibits faster capacity decay which is due to the consumption of FEC and active Li component[42]. Thus, the concentration of LiODFB and FEC in the DEEP-based electrolyte needs to be further explored to optimize the galvanostatic cycling performance in the following investigation.

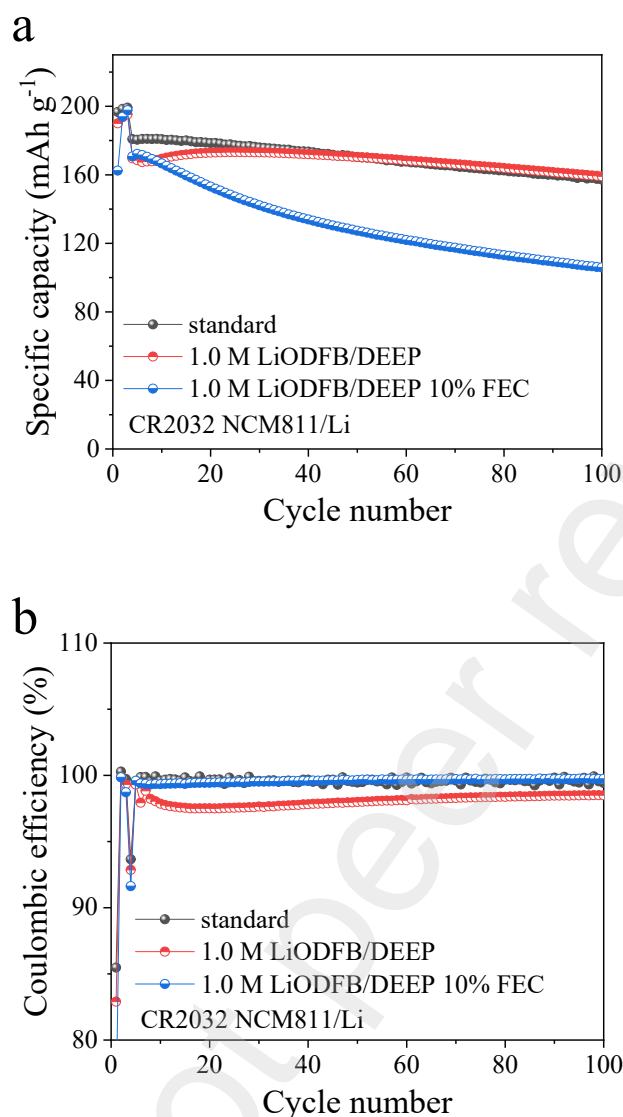


Fig.2 Cycling performance of NCM811 || Li coin cells using considered electrolytes (a: reversible specific discharge capacity, b: Coulombic efficiency)

The LiODFB concentration in the DEEP-based electrolyte was firstly explored with a fixed FEC concentration of 10%, and the concentration of LiODFB was set as 0.8, 1.0, 1.1, 1.2, 1.3, 1.4 and 1.5 M, respectively. NCM811 || Li coin cells with a series of different electrolytes were pre-cycled 3 times at 0.2 C and thereafter cycled at 1.0 C for 100 cycles at 20 °C. Fig. 3 and Table 1 compare specific discharge capacity and Coulombic efficiency values. It can be seen that with the increase of LiODFB concentration, the

reversible specific discharge capacity increases until the LiODFB concentration reaches 1.3 M, the average specific discharge capacity of cells containing the 1.3 M LiODFB/DEEP 10% FEC electrolyte during 100 cycles is 149.95 mAh g⁻¹ with a capacity retention rate of 83.91% and average Coulombic efficiency of 99.58%. When the LiODFB concentration exceeds 1.3 M, the reversible specific discharge capacity of the cells decreases. This is because a higher lithium salt concentration will lead to an increase in the viscosity of the electrolyte, which is not conducive to the capacity[43, 44].

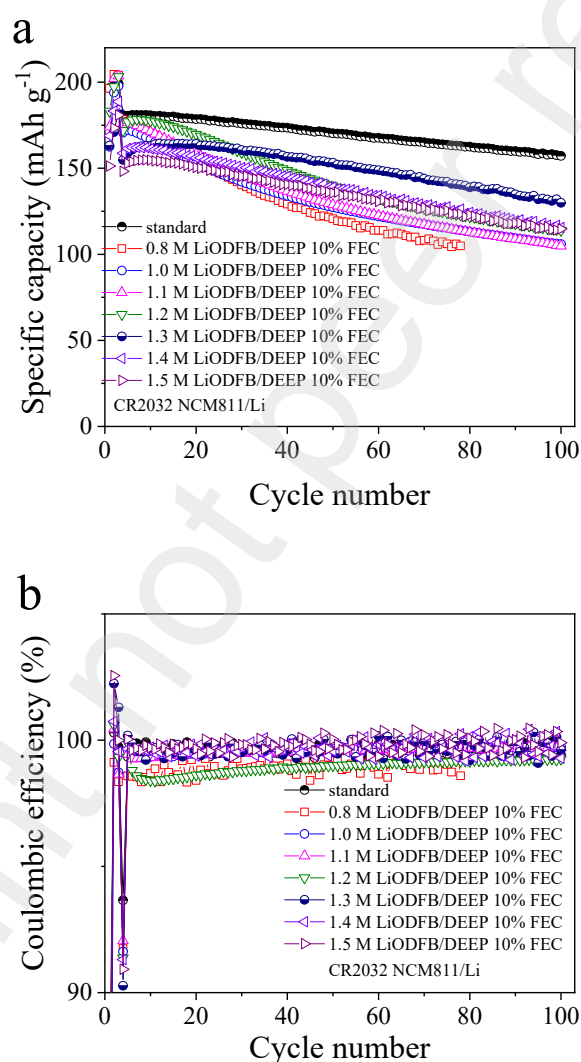


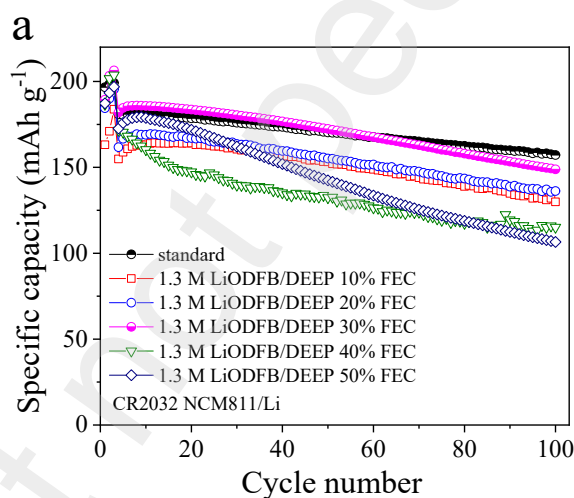
Fig.3 Galvanostatic cycling performance of NCM811 || Li coin cells containing standard and DEEP-based electrolytes with different concentration of LiODFB and 10% FEC. (a: reversible specific discharge capacity profiles, b: Coulombic efficiency)

Table 1 Specific discharge capacity, Coulombic efficiency and capacity retention of NCM811 || Li coin cells containing standard and DEEP-based electrolytes with different concentration of LiODFB and 10% FEC

Electrolyte formulation	Average specific discharge capacity (mAh g ⁻¹)	Initial Coulombic efficiency (%)	Average Coulombic efficiency (%)	Capacity retention rate (%)
Standard	169.48	86.77	99.54	86.90
0.8 M LiODFB/DEEP 10% FEC	\	\	\	\
1.0 M LiODFB/DEEP 10% FEC	130.14	61.35	99.53	62.04
1.1 M LiODFB/DEEP 10% FEC	131.91	59.28	99.49	59.74
1.2 M LiODFB/DEEP 10% FEC	141.60	65.58	98.89	66.28
1.3 M LiODFB/DEEP 10% FEC	149.95	83.72	99.58	83.91
1.4 M LiODFB/DEEP 10% FEC	138.11	72.17	99.60	72.78
1.5 M LiODFB/DEEP 10% FEC	134.45	86.77	99.73	77.42

After the optimal concentration of LiODFB was determined, the concentration of FEC was further optimized. The concentration of LiODFB was fixed at 1.3 M, and a

series of DEEP-based electrolytes with different concentrations (10%, 20%, 30%, 40% and 50%) of FEC were formulated. The galvanostatic cycling performance results are shown in Fig. 4 and Table 2. At concentration of FEC of 30 wt.% , the average specific discharge capacity of NCM811 || Li cells containing the 1.3 M LiODFB/DEEP 30% FEC electrolyte after 100 charge/discharge cycles amounts to 169.45 mAh g⁻¹, the capacity retention rate is 81.82%, and the average Coulombic efficiency is 99.53%, which is competent to cells containing standard electrolyte. When the concentration of FEC is further increased, the cycling performance of cells decreased, for the cells containing the 1.3 M LiODFB/DEEP 50% FEC electrolyte, the first Coulombic efficiency decreased to 60.85%, due to the fact that excessive FEC is not conducive to the construction of an effective SEI[45].



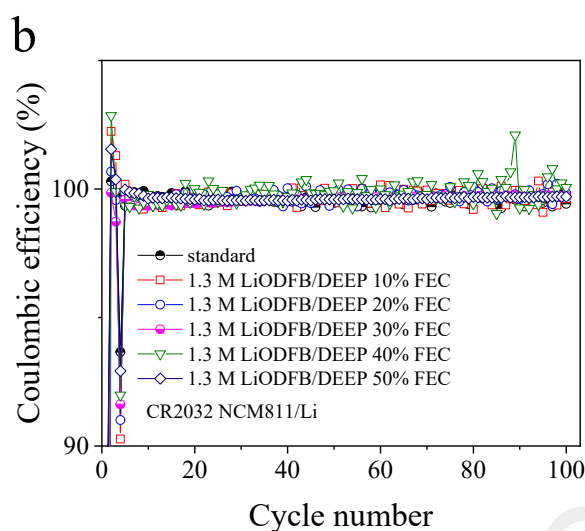


Fig. 4 Galvanostatic cycling performance of NCM811 || Li cells using standard and DEEP-based electrolytes with different concentration of FEC. (a: reversible specific discharge capacity profiles, b: Coulombic efficiency)

Table 2 Specific discharge capacity, Coulombic efficiency and capacity retention of NCM811 || Li coin cells using standard and DEEP-based electrolytes with different concentration of FEC

Electrolyte formulation	Average specific discharge capacity (mAh g ⁻¹)	Initial Coulombic efficiency (%)	Average Coulombic efficiency (%)	Capacity retention rate (%)
Standard	169.48	86.77	99.54	86.90
1.3 M LiODFB/DEEP 10% FEC	149.95	83.72	99.58	83.91
1.3 M LiODFB/DEEP 20% FEC	153.49	83.62	99.62	84.20
1.3 M LiODFB/DEEP 30% FEC	169.45	81.05	99.53	81.82

Electrolyte formulation	Average specific discharge capacity (mAh g⁻¹)	Initial Coulombic efficiency (%)	Average Coulombic efficiency (%)	Capacity retention rate (%)
FEC				
1.3 M LiODFB/DEEP 40%	132.33	64.70	99.75	67.11
FEC				
1.3 M LiODFB/DEEP 50%	141.36	60.85	99.57	61.74
FEC				

In order to further improve the electrochemical performance of cells containing the DEEP-based electrolyte, further concentration screening of FEC and LiODFB was conducted to identify the optimum electrolyte formulation. The concentration of LiODFB was explored again on the basis of a fixed FEC concentration at 30%. The cycling performance of cells containing 1.2 M LiODFB/DEEP 30% FEC, 1.3 M LiODFB/DEEP 30% FEC, 1.4 M LiODFB/DEEP 30% FEC and 1.5 M LiODFB/DEEP 30% FEC electrolytes is shown in Fig.5 (a-b). Cells containing the 1.3 M LiODFB/DEEP 30% FEC electrolyte exhibit the best electrochemical performance. By analyzing the specific discharge capacity and Coulombic efficiency values, the FEC and LiODFB concentration shows a synergistic effect on the galvanostatic cycling performance. To verify this synergistic effect, the concentrations of LiODFB and FEC were adjusted simultaneously to observe the influence on galvanostatic cycling performance. Fig. 5 (c-d) shows that the galvanostatic cycling performance of cells containing the 1.4 M LiODFB/DEEP 40% FEC electrolyte is quite close to that of cells containing 1.3 M LiODFB/DEEP 30% FEC electrolyte. This means that when the concentration ratio of FEC and LiODFB is appropriate, the cell performance can be better exerted. However, for cells containing the

1.5 M LiODFB DEEP 50% FEC and 1.6 M LiODFB/DEEP 60% FEC electrolytes, the galvanostatic cycling performance of cells degenerated obviously, which is closely related to the changes of the viscosity, ionic conductivity and complex interfacial reaction process of the electrolyte with a high concentration of FEC and LiODFB[43, 44].

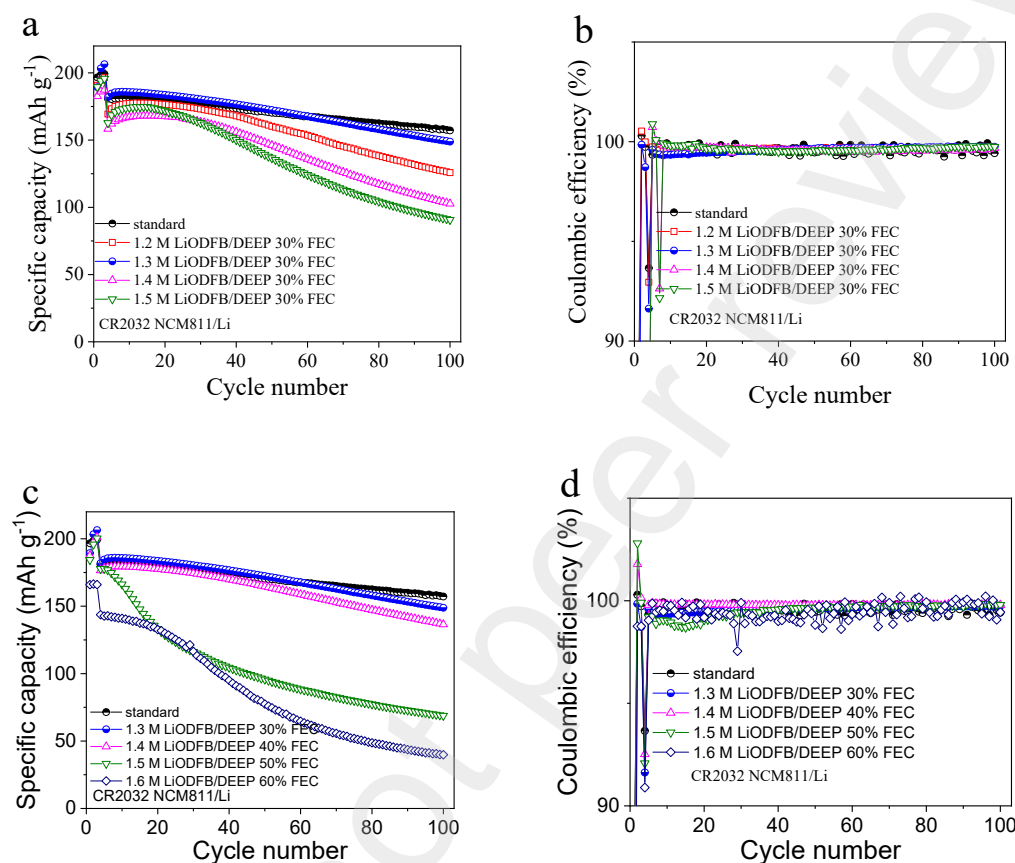


Fig.5 Galvanostatic cycling performance of NCM811 || Li coin cells using standard and DEEP-based electrolytes by concentration screening of LiODFB and FEC. (a, c: reversible specific discharge capacity profiles, b, d: Coulombic efficiency)

This study points out that the electrolyte formulation displaying optimized electrochemical performance is 1.3 M LiODFB/DEEP 30% FEC. The reversible specific discharge capacity and Coulombic efficiency of cells containing the 1.3 M LiODFB/DEEP 30% FEC electrolyte are comparable to commercial organic carbonate based electrolyte containing counterparts at a current rate of 1.0 C at 20 °C. The rate

performance of NCM811 || Li cells using standard and 1.3 M LiODFB/DEEP 30% FEC electrolytes at 20 °C is further compared in Fig.6. It can be seen that the rate performance of the 1.3 M LiODFB/DEEP 30% FEC electrolyte containing cell is, when the C-rate is lower than 1.0 C, the specific discharge capacity is quite close to the standard electrolyte counterpart. When the C-rate increases to 2.0 C, the discharge capacity of 1.3 M LiODFB/DEEP 30% FEC electrolyte containing cell significantly decreases, which may be limited by the lower ionic conductivity[46]. Table 3 compares the ionic conductivity of the standard electrolyte and 1.3 M LiODFB/DEEP 30% FEC electrolyte at 20 °C, 25 °C and 30 °C, respectively. At low C-rate, the ionic conductivity of electrolyte is not the main limiting factor for the electrochemical performance of cells containing DEEP-based electrolyte, whereas for a higher C-rate, since the ionic conductivity of the 1.3 M LiODFB/DEEP 30% FEC electrolyte is lower than for the standard electrolyte, its high rate performance in the considered cell is limited.

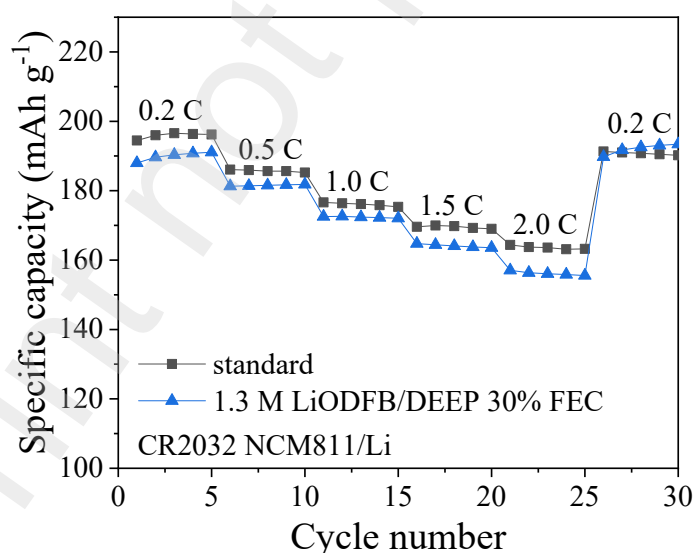
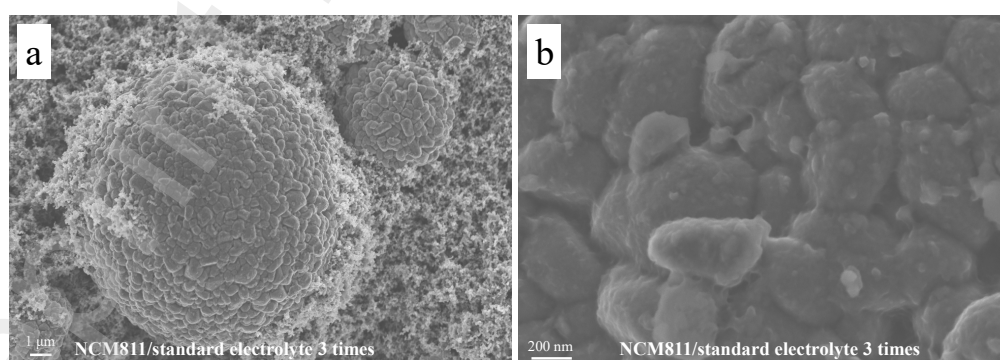


Fig.6 Rate performance test of NCM811-based cells using standard and 1.3 M LiODFB/DEEP 30% FEC electrolytes

Table 3 Ionic conductivity of standard and 1.3 M LiODFB/DEEP 30% FEC electrolytes at three different temperatures

Electrolyte formulation	Ionic conductivity (mS cm^{-1})		
	20 °C	25 °C	30 °C
Standard	5.4	5.9	6.5
1.3 M LiODFB/DEEP 30% FEC	2.7	3.1	3.5

SEM analysis of NCM811 electrodes disassembled from NCM811||Li cells containing standard and 1.3 M LiODFB/DEEP 30% FEC electrolytes after 3 and 100 charge/discharge cycles were conducted, respectively. The surface morphology of the NCM811 electrode is presented in Fig. 7. For cells containing 1.3 M LiODFB/DEEP 30% FEC electrolyte, no obvious electrolyte decomposition and deposition products were observed on the NCM811 electrode surface, which is consistent with cells containing the standard electrolyte. The adverse side electrochemical decomposition reactions of phosphate molecules are effectively suppressed[39], indicating that the NCM811||Li cells containing the optimized DEEP-based electrolyte display a similar electrochemical behavior with the cells containing standard electrolyte.



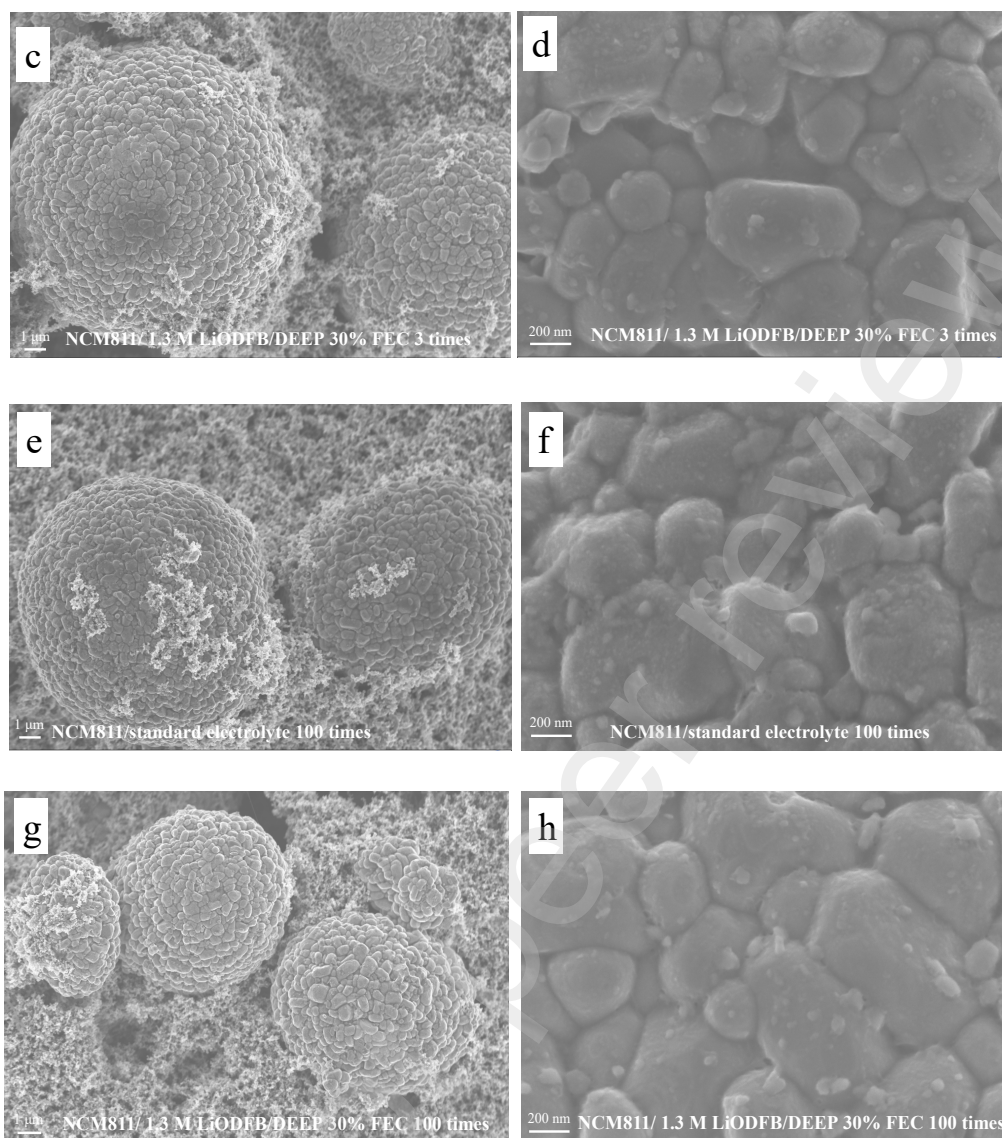


Fig. 7 Surface morphology of NCM811 electrode disassembled from NCM811 || Li cells containing standard (a-b, e-f), and 1.3 M LiODFB/DEEP 30% FEC (c-d, g-h) electrolytes after 3 and 100 cycles.

The original intention to design the DEEP-based electrolyte is to improve the safety of lithium-based batteries. Therefore, after optimization of electrolyte formulation with enhanced electrochemical performance, the safety of the 1.3 M LiODFB/DEEP 30% FEC electrolyte was investigated by means of self-extinguishing time (SET) determination and C80 microcalorimetry tests. Fig. 8a compares the flammability of the standard and 1.3 M

LiODFB/DEEP 30% FEC electrolytes by SET test. As can be seen that the standard electrolyte with organic carbonate solvent with low flash point can be easily ignited and highly flammable, whereas the 1.3 M LiODFB/DEEP 30% FEC electrolyte was hard to be ignited with a SET value of 0 s g^{-1} , indicating an excellent safety property.

In order to analyze the thermal stability of the DEEP-based electrolyte, the C80 microcalorimetry tests were further carried out on DEEP, LiODFB and FEC electrolyte components. Fig.8b shows heat flow variation of DEEP, LiODFB and FEC with the temperature increase. The peak heat flow temperature of LiODFB decomposition occurs at 240°C , which is higher than conventional LiPF_6 salt (196°C)[47]. The peak heat flow temperature of DEEP and FEC decomposition occur at 221°C and 259°C , respectively. Fig.8c compared the heat flow curves of commercial organic carbonate-based electrolyte (1.0 M $\text{LiPF}_6/\text{EC}/\text{DEC}$ (1:1 wt.%)[47] and 1.3 M LiODFB/DEEP 30% FEC electrolyte, the peak heat flow of DEEP-based electrolyte is lower than that of commercial electrolyte. More importantly, the electrolyte and the electrode coexist in the cell, and the thermal reactions of the electrode wetted with considered electrolyte significantly affects the cell safety. In Fig. 8d, the heat flow curve of the NCM811 electrode wetted with organic carbonate-based electrolyte shows a sharp exothermic peak with a high peak heat flow of 172 m W g^{-1} [39]. While the peak heat flow of the NCM811 electrode wetted with 1.3 M LiODFB/DEEP 30% FEC electrolyte during the programmed heating test is 40 mW g^{-1} , which is much milder than the commercial cell system. Obtained results pointed out that the 1.3 M LiODFB/DEEP 30% FEC electrolyte is nonflammable in nature and exhibits low heat generation during thermal decomposition, thus significantly reducing the thermal decomposition reactivity of the NCM811 electrode wetted with electrolyte to improve cell safety.

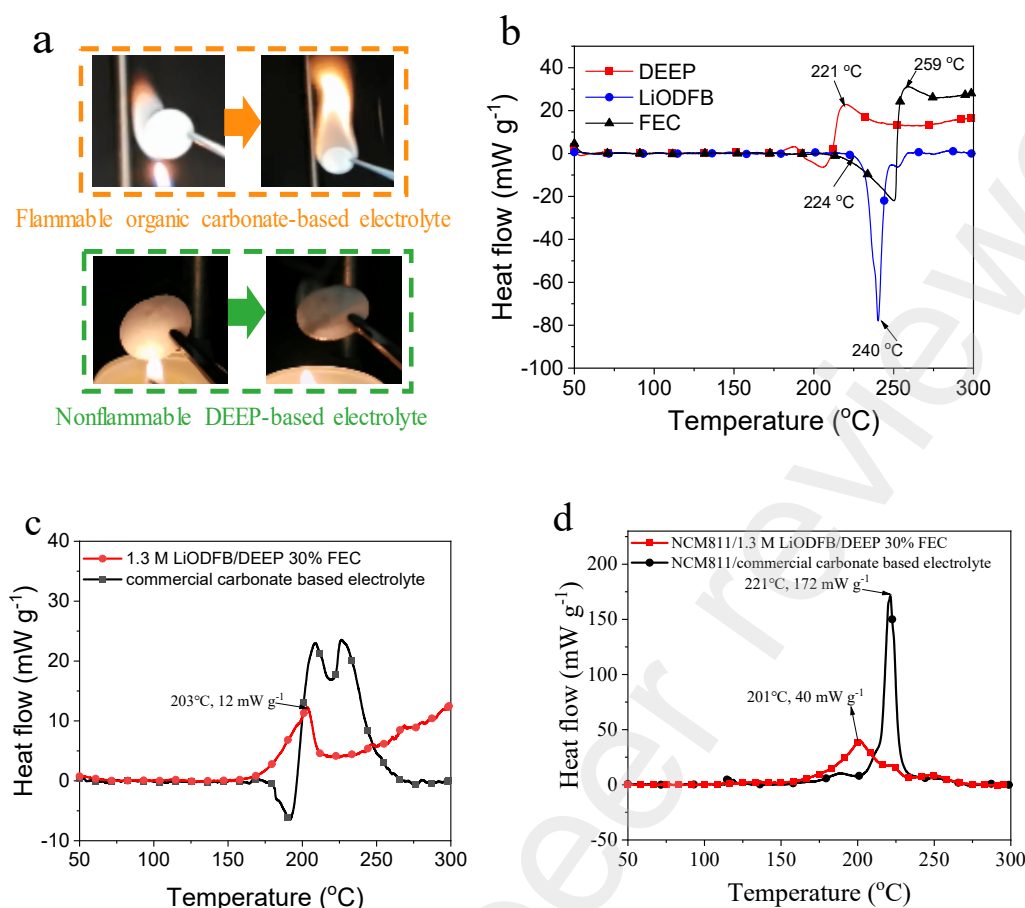


Fig. 8. (a) SET test of standard electrolyte and 1.3 M LiODFB/DEEP 30% FEC electrolyte, (b-d) heat flow vs. temperature dependence of DEEP, LiODFB, DEEP, 1.3 M LiODFB/DEEP 30% FEC electrolyte, and NCM811 electrode wetted with 1.3 M LiODFB/DEEP 30% FEC electrolyte compared to commercial organic carbonate electrolyte-based cell[39, 47]

4. Conclusions

In summary, a novel electrolyte formulation with LiODFB as lithium conducting salt, DEEP flame retardant as the main solvent and FEC as the co-solvent was designed and evaluated in NCM811 || Li cells. The optimized DEEP-based electrolyte containing cells show both competent electrochemical performance and excellent safety performance. For electrochemical performance, LiODFB and FEC exhibit a synergistic effect by regulating the reversible specific discharge capacity and Coulombic efficiency. The

identified 1.3 M LiODFB/DEEP 30% FEC formulation improves the galvanostatic cycling and the rate performance of NCM811 || Li cells to a comparable level compared to commercial organic carbonate electrolytes. In addition, the DEEP-based electrolyte is nonflammable in nature displaying higher thermal stability and reduces the thermal decomposition reactivity of the NCM811 electrode. Thus, the 1.3 M LiODFB/DEEP 30% FEC electrolyte is recommended as a good potential candidate for improving the safety of the next generation of lithium-based batteries.

Conflicts of interest

There are no conflicts to declare.

Acknowledgements

This work was supported by the National Natural Science Foundation of China (No. 52204248) and the China Postdoctoral Science Foundation (No. 2021M703053, No. 2022T150622). Q.S.W. was supported by Youth Innovation Promotion Association CAS (No. Y201768). L.H.J was supported by a scholarship (No. 201906340115) from China Scholarship Council (CSC).

References

- [1] B. Diouf, R. Podes, Potential of lithium-ion batteries in renewable energy, *Renewable Energy*, 76 (2015) 375-380.
- [2] A. Masias, J. Marcicki, W.A. Paxton, Opportunities and challenges of lithium ion batteries in automotive applications, *ACS energy letters*, 6 (2021) 621-630.
- [3] A. Manthiram, An outlook on lithium ion battery technology, *ACS central science*, 3 (2017) 1063-1069.
- [4] E. Fan, L. Li, Z. Wang, J. Lin, Y. Huang, Y. Yao, R. Chen, F. Wu, Sustainable recycling technology for Li-ion batteries and beyond: challenges and future prospects, *Chemical reviews*, 120 (2020) 7020-7063.

- [5] B. Xu, J. Lee, D. Kwon, L. Kong, M. Pecht, Mitigation strategies for Li-ion battery thermal runaway: A review, *Renewable and Sustainable Energy Reviews*, 150 (2021) 111437 (1-23).
- [6] S. Chen, Z. Gao, T. Sun, Safety challenges and safety measures of Li-ion batteries, *Energy Science & Engineering*, 9 (2021) 1647-1672.
- [7] G. Xu, L. Huang, C. Lu, X. Zhou, G. Cui, Revealing the multilevel thermal safety of lithium batteries, *Energy Storage Materials*, 31 (2020) 72-86.
- [8] Q.-K. Zhang, X.-Q. Zhang, H. Yuan, J.-Q. Huang, Thermally stable and nonflammable electrolytes for lithium metal batteries: progress and perspectives, *Small Science*, 1 (2021) 2100058 (1-14).
- [9] X. Feng, S. Zheng, D. Ren, X. He, L. Wang, H. Cui, X. Liu, C. Jin, F. Zhang, C. Xu, Investigating the thermal runaway mechanisms of lithium-ion batteries based on thermal analysis database, *Applied energy*, 246 (2019) 53-64.
- [10] Q. Wang, L. Jiang, Y. Yu, J. Sun, Progress of enhancing the safety of lithium ion battery from the electrolyte aspect, *Nano Energy*, 55 (2019) 93-114.
- [11] X. Feng, M. Ouyang, X. Liu, L. Lu, Y. Xia, X. He, Thermal runaway mechanism of lithium ion battery for electric vehicles: A review, *Energy Storage Materials*, 10 (2018) 246-267.
- [12] J. Chen, A. Naveed, Y. Nuli, J. Yang, J. Wang, Designing an intrinsically safe organic electrolyte for rechargeable batteries, *Energy Storage Materials*, 31 (2020) 382-400.
- [13] X. Tian, Y. Yi, B. Fang, P. Yang, T. Wang, P. Liu, L. Qu, M. Li, S. Zhang, Design strategies of safe electrolytes for preventing thermal runaway in lithium ion batteries, *Chemistry of Materials*, 32 (2020) 9821-9848.

- [14] K. Zhang, Y. An, C. Wei, Y. Qian, Y. Zhang, J. Feng, High-Safety and Dendrite-Free Lithium Metal Batteries Enabled by Building a Stable Interface in a Nonflammable Medium-Concentration Phosphate Electrolyte, *ACS Applied Materials & Interfaces*, 13 (2021) 50869-50877.
- [15] Y.-K. Sun, Promising all-solid-state batteries for future electric vehicles, in, *ACS Publications*, 2020, pp. 3221-3223.
- [16] Y. Yamada, J. Wang, S. Ko, E. Watanabe, A. Yamada, Advances and issues in developing salt-concentrated battery electrolytes, *Nature Energy*, 4 (2019) 269-280.
- [17] Y. Dong, N. Zhang, C. Li, Y. Zhang, M. Jia, Y. Wang, Y. Zhao, L. Jiao, F. Cheng, J. Xu, Fire-retardant phosphate-based electrolytes for high-performance lithium metal batteries, *ACS Applied Energy Materials*, 2 (2019) 2708-2716.
- [18] Z. Lu, L. Yang, Y. Guo, Thermal behavior and decomposition kinetics of six electrolyte salts by thermal analysis, *Journal of power sources*, 156 (2006) 555-559.
- [19] Y.-P. Yang, A.-C. Huang, Y. Tang, Y.-C. Liu, Z.-H. Wu, H.-L. Zhou, Z.-P. Li, C.-M. Shu, J.-C. Jiang, Z.-X. Xing, Thermal stability analysis of lithium-ion battery electrolytes based on lithium bis (trifluoromethanesulfonyl) imide-lithium difluoro (oxalato) borate dual-salt, *Polymers*, 13 (2021) 707 (1-12).
- [20] Z. Zeng, V. Murugesan, K.S. Han, X. Jiang, Y. Cao, L. Xiao, X. Ai, H. Yang, J.-G. Zhang, M.L. Sushko, Non-flammable electrolytes with high salt-to-solvent ratios for Li-ion and Li-metal batteries, *Nature Energy*, 3 (2018) 674-681.
- [21] J. Wang, Y. Yamada, K. Sodeyama, E. Watanabe, K. Takada, Y. Tateyama, A. Yamada, Fire-extinguishing organic electrolytes for safe batteries, *Nature Energy*, 3 (2018) 22-29.

- [22] X. Wang, W. He, H. Xue, D. Zhang, J. Wang, L. Wang, J. Li, A nonflammable phosphate-based localized high-concentration electrolyte for safe and high-voltage lithium metal batteries, *Sustainable Energy & Fuels*, 6 (2022) 1281-1288.
- [23] Z. Wang, H. Zhang, J. Xu, A. Pan, F. Zhang, L. Wang, R. Han, J. Hu, M. Liu, X. Wu, Advanced Ultralow-Concentration Electrolyte for Wide-Temperature and High-Voltage Li-Metal Batteries, *Advanced Functional Materials*, (2022) 2112598 (1-9).
- [24] S. Chen, J. Zheng, L. Yu, X. Ren, M.H. Engelhard, C. Niu, H. Lee, W. Xu, J. Xiao, J. Liu, High-efficiency lithium metal batteries with fire-retardant electrolytes, *Joule*, 2 (2018) 1548-1558.
- [25] S. Chen, J. Zheng, D. Mei, K.S. Han, M.H. Engelhard, W. Zhao, W. Xu, J. Liu, J.G. Zhang, High-voltage lithium-metal batteries enabled by localized high-concentration electrolytes, *Advanced materials*, 30 (2018) 1706102 (1-7).
- [26] B.S. Parimalam, B.L. Lucht, Reduction reactions of electrolyte salts for lithium ion batteries: LiPF₆, LiBF₄, LiDFOB, LiBOB, and LiTFSI, *Journal of The Electrochemical Society*, 165 (2018) A251-A255.
- [27] K. Zhang, Y. Tian, C. Wei, Y. An, J. Feng, Building stable solid electrolyte interphases (SEI) for micro-sized silicon anode and 5V-class cathode with salt engineered nonflammable phosphate-based lithium-ion battery electrolyte, *Applied Surface Science*, 553 (2021) 149566.
- [28] Y. Wang, H. Zheng, L. Hong, F. Jiang, Y. Liu, X. Feng, R. Zhou, Y. Sun, H. Xiang, Lithium difluoro (bisoxalato) phosphate-based multi-salt low concentration electrolytes for wide-temperature lithium metal batteries: Experiments and theoretical calculations, *Chemical Engineering Journal*, 445 (2022) 136802.

- [29] S.S. Zhang, An unique lithium salt for the improved electrolyte of Li-ion battery, *Electrochemistry communications*, 8 (2006) 1423-1428.
- [30] C. Liu, Q. Huang, K. Zheng, J. Qin, D. Zhou, J. Wang, Impact of lithium salts on the combustion characteristics of electrolyte under diverse pressures, *Energies*, 13 (2020) 5373 (1-15).
- [31] Q. Zhang, Z. Wang, X. Li, H. Guo, J. Wang, G. Yan, Unraveling the role of LiODFB salt as a SEI-forming additive for sodium-ion battery, *Ionics*, 27 (2021) 683-691.
- [32] Y. Liu, J. Wu, Y. Yang, A Double-Layer Artificial SEI Film Fabricated by Controlled Electrochemical Reduction of LiODFB-FEC Based Electrolyte for Dendrite-Free Lithium Metal Anode, *Journal of The Electrochemical Society*, 167 (2020) 160535 (1-10).
- [33] H. Chen, B. Liu, Y. Wang, H. Guan, H. Zhou, Insight into wide temperature electrolyte based on lithiumdifluoro (oxalate) borate for high voltage lithium-ion batteries, *Journal of Alloys and Compounds*, 876 (2021) 159966 (1-13).
- [34] J. Yu, N. Gao, J. Peng, N. Ma, X. Liu, C. Shen, K. Xie, Z. Fang, Concentrated LiODFB electrolyte for lithium metal batteries, *Frontiers in chemistry*, 7 (2019) 494 (1-8).
- [35] Z. Xu, J. Wang, J. Yang, X. Miao, R. Chen, J. Qian, R. Miao, Enhanced performance of a lithium–sulfur battery using a carbonate-based electrolyte, *Angewandte chemie international edition*, 55 (2016) 10372-10375.
- [36] M. Tao, Y. Xiang, D. Zhao, P. Shan, Y. Sun, Y. Yang, Quantifying the Evolution of Inactive Li/Lithium Hydride and Their Correlations in Rechargeable Anode-free Li Batteries, *Nano Letters*, 22 (2022) 6775-6781.

- [37] K. Oldiges, N. von Aspern, I. Cekic-Laskovic, M. Winter, G. Brunklaus, Impact of trifluoromethylation of adiponitrile on aluminum dissolution behavior in dinitrile-based electrolytes, *Journal of The Electrochemical Society*, 165 (2018) A3773-A3781.
- [38] S. Fletcher, I. Kirkpatrick, R. Thring, R. Dring, J.L. Tate, H.R. Geary, V.J. Black, Ternary mixtures of sulfolanes and ionic liquids for use in high-temperature supercapacitors, *ACS Sustainable Chemistry & Engineering*, 6 (2018) 2612-2620.
- [39] L. Jiang, C. Liang, H. Li, Q. Wang, J. Sun, Safer triethyl-phosphate-based electrolyte enables nonflammable and high-temperature endurance for a lithium ion battery, *ACS Applied Energy Materials*, 3 (2020) 1719-1729.
- [40] K. Matsumoto, K. Inoue, K. Utsugi, A highly safe battery with a non-flammable triethyl-phosphate-based electrolyte, *Journal of Power Sources*, 273 (2015) 954-958.
- [41] X.Q. Zhang, X.B. Cheng, X. Chen, C. Yan, Q. Zhang, Fluoroethylene carbonate additives to render uniform Li deposits in lithium metal batteries, *Advanced Functional Materials*, 27 (2017) 1605989 (1-8).
- [42] R. Jung, M. Metzger, D. Haering, S. Solchenbach, C. Marino, N. Tsiouvaras, C. Stinner, H.A. Gasteiger, Consumption of fluoroethylene carbonate (FEC) on Si-C composite electrodes for Li-ion batteries, *Journal of The Electrochemical Society*, 163 (2016) A1705-A1716.
- [43] X. Ren, S. Chen, H. Lee, D. Mei, M.H. Engelhard, S.D. Burton, W. Zhao, J. Zheng, Q. Li, M.S. Ding, Localized high-concentration sulfone electrolytes for high-efficiency lithium-metal batteries, *Chem*, 4 (2018) 1877-1892.
- [44] M.S. Ding, A. von Cresce, K. Xu, Conductivity, viscosity, and their correlation of a super-concentrated aqueous electrolyte, *The Journal of Physical Chemistry C*, 121 (2017) 2149-2153.

- [45] A. Bouibes, N. Takenaka, K. Kubota, S. Komaba, M. Nagaoka, Development of advanced electrolytes in Na-ion batteries: application of the Red Moon method for molecular structure design of the SEI layer, *RSC advances*, 12 (2022) 971-984.
- [46] S. Zhang, J. Li, N. Jiang, X. Li, S. Pasupath, Y. Fang, Q. Liu, D. Dang, Rational Design of an Ionic Liquid-Based Electrolyte with High Ionic Conductivity Towards Safe Lithium/Lithium-Ion Batteries, *Chemistry—An Asian Journal*, 14 (2019) 2810-2814.
- [47] L. Jiang, Q. Wang, K. Li, P. Ping, L. Jiang, J. Sun, A self-cooling and flame-retardant electrolyte for safer lithium ion batteries, *Sustainable Energy & Fuels*, 2 (2018) 1323-1331.